Stepwise Solvatochromism of Ketyl Anions in the Gas Phase: Photodetachment Excitation Spectroscopy of Benzophenone and Acetophenone Radical Anions Microsolvated with Methanol†

Izumi Yagi, Toshihiko Maeyama,* Asuka Fujii, and Naohiko Mikami*

Department of Chemistry, Graduate School of Science, Tohoku University, Aoba-ku, Sendai 980-8578, Japan

Received: March 19, 2007; In Final Form: May 10, 2007

Electronic absorption spectra of bare and methanol-solvated radical anions of benzophenone ($(C_6H_5)_2CO$) and acetophenone ($(C_6H_5)CH_3CO$) were measured by monitoring the photodetachment efficiency in the gas phase. Strong absorption bands due to autodetachment after transitions to bound excited states were observed. Stepwise spectral shifts approaching the limit of the condensed phase spectra were found to occur as the cluster size increases. In the case of benzophenone radical anion, the solvation of two methanol molecules exhibits the near convergence to the limit, representing the full coordination with the solvent molecules around the carbonyl group. For the acetophenone case, the coordination number was not apparently determined because of their relatively small shifts. Relationships between hydrogen bonding and electronic structure are analyzed for the spectral shifts with the aid of calculations based on density functional theory. The calculational results show that the coordination angle of the solvent molecule is affected mostly by steric hindrance around the carbonyl group, and that there is no evidence for reorientation due to specific hydrogen bonding interaction with the singly occupied orbital, which has been formerly persisted for an interpretation of the transient absorption following pulse radiolysis in alcoholic solutions. An alternative possibility involving deformation with respect to intramolecular coordinates is discussed.

1. Introduction

Radical anions of aromatic carbonyl compounds (so-called ketyl anions) have been shown great interest as an intermediate species in numerous reductive reactions induced by alkali metal addition,[1,2] electrolysis,[3,4] flash photolysis,[5,6] pulse radiolysis,[7−12] and γ radiolysis.[13−16] The solvent effect investigation on their visible absorption bands has a long history for over 70 years, since Bachmann[2] reported the solvent-dependent chromatic change of alkali-reduced ketone solutions in 1933. After 30 years, Shida and Hamill[13] observed for the first time the metal-free absorption spectra of several ketyl anions in various matrices using γ radiolysis, where the absorption maxima in protic solvents (e.g., ethanol) exhibited a large blue-shift compared to those in aprotic solvents such as diethylether or 2-methyltetrahydrofuran (2-MTHF). The absorption bands have been assigned to the intramolecular charge-transfer (ICT) band between the antibonding orbitals of the carbonyl group and the aromatic ring(s). The blue-shift in protic solvents was considered to originate from the stabilization of the ground-state energy level due to hydrogen bond formation around the anionic carbonyl group. Transient absorption spectra of benzophenone radical anion (Bp^-) generated by pulse radiolysis in various alcoholic solutions[9−12] have been intensively studied with respect to solvent reorientation dynamics following electron capture of the neutral benzophenone. Ichikawa and co-workers[15] measured absorption spectra of Bp^- in mixed solvents of ethanol and 2-MTHF under several concentration conditions. They fitted the spectra to a superposition of three components representing coordination number of ethanol molecules (n = 0, 1, and 2) and concluded that two ethanol molecules can attach to the carbonyl group. However, there is still an ambiguity for the analysis because arbitrary functions can be chosen for the spectral components as long as the maximum coordination number is presumed.

At the present time, the most unambiguous way to examine the molecular scale interaction in hydrogen-bonded systems is spectroscopy of size-selected clusters. Electronic absorption spectra of microsolvated anions are significant because they can be compared directly with a large number of spectra in the condensed phase. Electron affinity of an isolated molecule or a small cluster is generally small (<1 eV) so that most bound electronic excited states of the anions will release the excess electron automatically through nonadiabatic or electron correlation effects. Photoabsorption cross-section for a bound−bound transition tends to be much larger than that for bound-free transition of direct electron detachment. Hence, transitions to a bound electronic state above the detachment threshold will appear in a spectrum monitoring the photodetachment efficiency (PDE). In this work, we report PDE spectra of bare and methanol-solvated radical anions of benzophenone ($Bp^-\cdot(MeOH)_n$, n = 0−5) and acetophenone ($Ap^-\cdot(MeOH)_n$, n = 0−4). On the basis of the observed spectra, we discuss the coordination mechanism of methanol molecules around the ketyl anions as well as the electronic structures of the anions with the aid of quantum chemical calculations using density functional theory.

2. Experimental and Computational Methods

Experimental setups in this work are similar to those described elsewhere.[17,18] Electrons photoemitted from Zr metal surface were attached to neutral clusters prepared in a supersonic expansion of sample vapor seeded in argon gas at 2 atm of

† Part of the "Roger E. Miller Memorial Issue".

* To whom correspondence should be addressed. E-mail: tmaeyama@mail.tains.tohoku.ac.jp (T.M.).

10.1021/jp072167l CCC: $37.00
Published on Web 06/13/2007

stagnation pressure. For benzophenone, the pulsed beam source including a sample container was heated up to 120 °C to gain a sufficient vapor pressure. The anions were repelled into a drift tube of a time-of-flight mass spectrometer by a high-voltage electric pulse. When target mass species reached the photointeraction region in the middle of the drift tube, they were irradiated by a light pulse from the signal or idler output of an optical parametric oscillator (OPO; GWU-Lasertechnik, VisIR2). Photodetached electrons were collected into a closely placed microchannel plate by an electric pulse of −15 V. Signal intensities of the target anions and the electrons were simultaneously monitored by a digital oscilloscope (Lecroy, Waverunner 6050) connected via a GPIB interface to a personal computer. The normalization of the electron signal intensity against the anion intensity was carried out. In addition, the light fluence (P) was synchronously monitored through a separate data acquisition card (NI 6251) in the computer. PDE at the photon energy (E) was obtained in arbitrary units by the normalization of the electron signal against the photon flux (P/E).

All of the quantum chemical calculations in this study were based on density functional theory (DFT), and also time-dependent density functional theory (TDDFT) was applied for calculations of electronic transitions to excited states. The calculations were performed by the Gaussian 03 program suite[19] using the B3LYP level of theory with the 6-31+(d,p) basis set. The Molden[20] and Molekel[21] programs were used for visualization of molecular models.

3. Results and Discussion

Bare and Methanol-Solvated Benzophenone Radical Anions. Figure 1 shows the PDE spectra of the bare and methanol-solvated benzophenone anion ($Bp^-\cdot(MeOH)_n$, $n = 0-5$). The electron affinity of benzophenone[22−24] has been reported to be 0.63 ± 0.02 eV. For the bare anion ($n = 0$), weak electron signals due to the direct detachment were detected in the range of 0.7−1.0 eV. However, the PDE of Bp^- exhibits a sudden rise at around 1.10 eV, which corresponds to the band origin of an electronic transition to an excited bound state. Similarly to the absorption spectrum in a cold 2-MTHF matrix,[13−16] the present spectrum of Bp^- in the gas phase shows no vibrational structure, suggesting a large deformation upon the excitation and/or a short lifetime in the excited state. The peak of the band at 1.43 ± 0.04 eV is 0.08 eV lower than that of the absorption spectrum in the matrix, of which the molar absorption coefficient[16] was reported to be approximately 10^4 $dm^3 \cdot cm^{-1} \cdot mol^{-1}$. Assuming that the autodetachment cross-section in the gas phase is similar to the photoabsorption cross-section in the condensed phase, it can be estimated to be on the order of 10^{-17} cm^2. The direct detachment cross-section at the absorption peak is as small as that with a factor less than 10^{-1}.

In Figure 1, the dependence of the solvation of methanol molecules ($n = 0-5$) is shown, representing remarkable shifts to the higher energy side with an increase of the cluster size. Additivity of the large shift of 0.17 eV stands for $n = 2$, while the increment of the shifts for $n \geq 3$ is apparently reduced. The PDE spectrum for $n = 5$ is almost equivalent to the absorption spectrum in bulk ethanol, which is supposed to be similar to the methanol system. Several isomers of different coordination numbers were found for $n \geq 2$ in geometry optimization of the DFT calculations. However, The most stable structures of $Bp^-\cdot(MeOH)_n$, $n = 1-3$, are shown in Figure 2, where up to two methanol molecules are bound directly to the carbonyl group, but the third one forms a hydrogen bond chain with the other one. The structure of triple coordination is found to be unstable for $n = 3$. The directly bound methanols overhang the plane defined by the two C−C bonds between the carbonyl and phenyl groups. The TDDFT calculations for $n = 0-3$ reveal several electronic transitions with different vertical transition energies as well as oscillator strengths in this region, which are appended in Figure 1. Although the absolute transition energies are larger than the experimental values, trends in the energy shift at each solvation step are reproduced. Thus, the maximum coordination number of methanol to the carbonyl group of Bp^- is unambiguously determined to be two, which is identical with that predicted in the study of Ichikawa et al. We will discuss later details of the electronic and geometric structures of Bp^- giving rise to the nature of methanol coordination and spectral shifts.

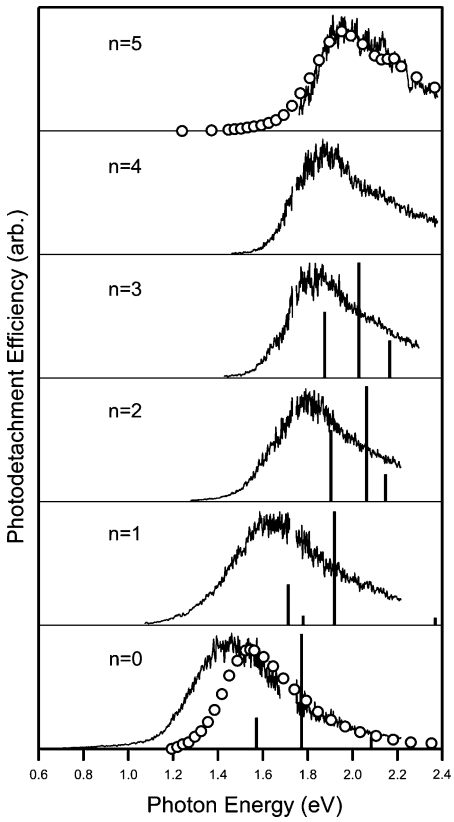

Figure 1. PDE spectra of $Bp^-\cdot(MeOH)_n$, $n = 0-5$. Spectral gaps around 1.7 eV are caused by insufficient fluence of the OPO output. Oscillator strengths at theoretical transition energies are appended as stick graphs for $n = 0-3$. The condensed phase absorption spectra (ref 13) in 2-MTHF and in ethanol are exhibited as open squares on the bottom and top panels, respectively.

Bare and Methanol-Solvated Acetophenone Radical Anions. The electron affinity of acetophenone[25] has been reported to be 0.334 ± 0.006 eV. Figure 3 shows the PDE spectra of bare and methanol-solvated acetophenone anions ($Ap^-\cdot(MeOH)_n$, $n = 0-4$). Broad absorption bands in the range of 2.2−3.0 eV are attributed to transitions to autodetaching bound states. In the energy region lower than 2.2 eV, there are considerable backgrounds that might be mainly due to direct detachment, although weak absorption bands involving low-lying bound states were observed in a 2-MTHF matrix.[13,16] The direct electron detachment cross-section for Ap^- is large compared to that for Bp^- because their peak absorption coefficients were reported to be on the same order. The absorption peak for the bare anion appears at 2.55 ± 0.03 eV, which is very close to that in the bulk system. Shoulders due to vibrational structure

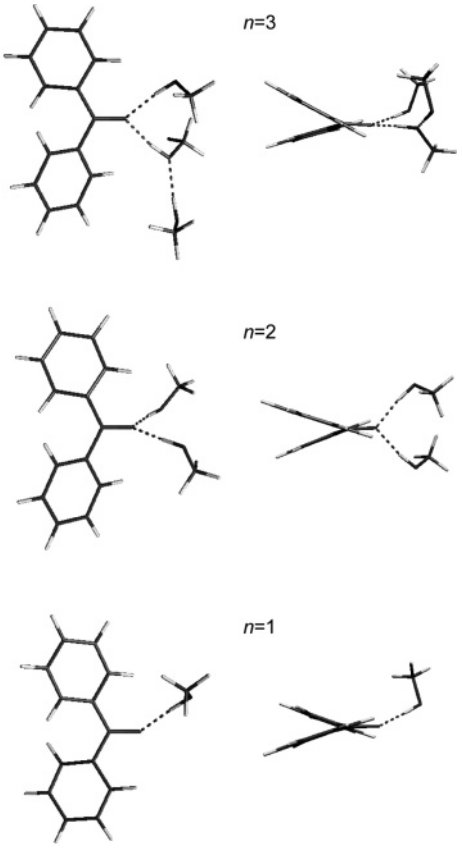

Figure 2. Optimized structures of $Bp^-\cdot(MeOH)_n$, $n = 0-3$ at the B3LYP/6-31+G(d,p) level in top (left) and side (right) views.

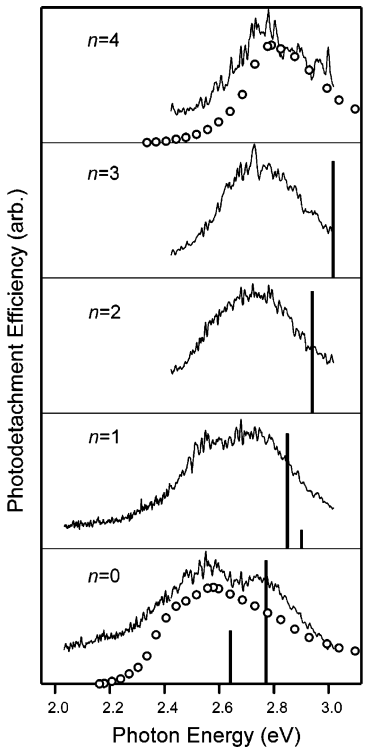

Figure 3. PDE spectra of $Ap^-\cdot(MeOH)_n$, $n = 0-4$. Oscillator strengths at theoretical transition energies are appended as stick graphs for $n = 0-3$. The condensed phase absorption spectra (ref 13) in 2-MTHF and in ethanol are exhibited as open squares on the bottom and top panels, respectively.

of the excited state appear at similar positions both in the gas and 2-MTHF matrix phases.

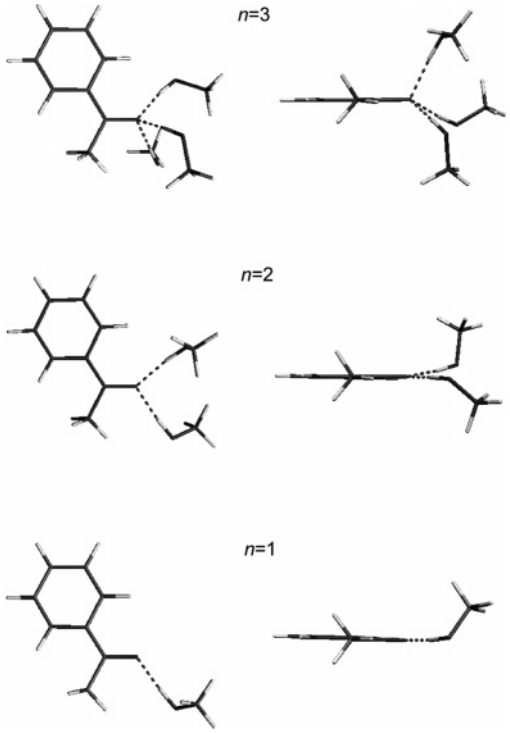

Figure 4. Optimized structures of $Ap^-\cdot(MeOH)_n$, $n = 0-3$ at the B3LYP/6-31+G(d,p) level in top (left) and side (right) views.

The peak position gradually shifts to the higher energy side as the cluster size increases. However, the peak shifts for the Ap^- system are much smaller than those for the Bp^- system, and there is no clear discontinuity of the size dependence. The PDE spectrum for $n = 4$ almost converges on the absorption spectrum in bulk ethanol. Figure 4 shows the geometric structures of $Ap^-\cdot(MeOH)_n$ for $n = 1-3$ optimized by the DFT calculations. Unlike the Bp^- system, the coordination of three methanol molecules around the carbonyl group was found. Vertical electronic transitions calculated for the bare and solvated anions are appended in Figure 3, where almost equivalent shifts of the transition energy are found to occur up to $n = 3$. The absolute values of the transition energy are overestimated by the TDDFT calculations, similar to the Bp^- case. It might be caused by the overestimation of the electron binding energy in the ground state because the B3LYP level of calculations with the basis set of 6-31+G(d,p) or larger often provide higher vertical detachment energies for hydrogen-bonded radical anion systems.[17,26] However, trends in the spectral shifts seem to acceptably reproduce the experimental results.

Fate of the Spectral Shifts at the Larger Cluster Sizes. The stepwise spectral shifts for the size-selected cluster anions are evidently due to differences between solvation energies in the ground and excited states. The differences are dominantly caused by a change of charge distributions in the anions upon the electronic transition. When the cluster size becomes large enough, the outer solvent molecules will recognize the anion as a point charge regardless of its charge distribution. Nevertheless, evolution of the spectral shift terminates at this limit, beyond which the increase of the solvation energy still continues as a charge−dielectric interaction. The classical cavity model of ionic solvation (known as the Born model[27,28]) may be applied to estimate the bulk solvation energy quantitatively, presuming the cavity size is identical with the volume of the cluster at the limit size.

The observed spectra with a few methanol molecules seem to have reached close proximity of the limit size for the solvation

energy independent of the electronic states. However, experimental spectra monitoring the PDE will evolve with an increase of the size beyond the limit, although we could not obtain the spectra for the larger sizes because of lack of sensitivity for the measurements. The stepwise solvation energy for the anionic excited-state involving charge-induced interactions should be larger than that for the corresponding neutral state. Thus, the excited-state energy becomes lower than the detachment threshold at a certain size. When the detachment threshold is close to the absorption band origin, the electron detachment channel should compete with another destruction channel such as dissociation following internal conversion to the anionic ground state. It should be pointed out that there is a possibility for the present PDE spectra of cluster anions to be affected by such a competition in the lower energy region. To measure a much more precise absorption spectrum for a large cluster anion, quantum yields for the destruction channels should be determined. Otherwise, other experimental techniques (e.g., excitation spectroscopy monitoring the photoneutrals or depletion spectroscopy of the target anion) will be applied for the total absorption cross-section measurements although they have much less sensitivity.

Electronic and Geometric Structures of the Ketyl Anions. Before discussing the molecular mechanism of solvatochromic shifts of the ketyl anions, electronic and geometric structures of the bare anions should be characterized by the results of DFT calculations. Figures 5 and 6 represent outer valence molecular orbitals of the α spin space simulated by DFT calculations for Bp^- and Ap^-, respectively. The 49th orbital for Bp^- and the 33rd orbital for Ap^- are assigned to their singly occupied molecular orbitals (SOMOs). The largest amplitudes of SOMO are found on the carbonyl group for both of the anions, but the phenyl ring of Ap^- exhibits relatively large amplitudes in the SOMO. The orbitals just below the SOMOs are attributed to the nonbonding orbitals, which play an important role for the hydrogen bond formation. The nonbonding orbitals are well localized on the horizontal sides of the carbonyl group, whereas the SOMOs spread over the whole molecules. According to natural population analyses for the neutral and anionic states (see Supporting Information), 36−37% of the excess charge is distributed on the carbonyl group both for Bp^- and Ap^-, and the rest is distributed among the phenyl ring(s).

The major difference on the geometrical aspect between the two ketyl anions is due to torsional angles of the phenyl rings with respect to the carbonyl group. The torsional angle for the neutral benzophenone is 28.4°, where the two rings twist to the opposite directions. On the other hand, Bp^- has a near planar structure in which the torsional angle reduces to 17.2°. For the acetophenone molecule, the geometry is optimized to be planar (except the hydrogen atoms of the methyl group) both in the neutral and anionic states. The phenyl torsion is related to the conjugation of π electrons as well as the repulsion between the substituents. The π conjugation predominantly affects the stabilization for the neutral and anionic acetophenone, having less steric hindrance due to the methyl group. For the neutral benzophenone, the repulsion between the two hydrogen atoms of the ortho position in the phenyl rings causes the torsion. In the anionic state, however, the more planar geometry results in the excess π electron on the phenyl rings with the more π conjugation.

Table 1 lists electronic transitions to bound excited states for Bp^- and Ap^- simulated by TDDFT calculations, where transitions of oscillator strength less than 0.01 are dismissed. The dominant contribution to the visible absorption of Bp^- is due to the excitations from the SOMO to the 51st and 53rd orbitals, of which electron distribution concentrates on the phenyl rings. In this respect, it is true for Bp^- that the absorption band is attributed to the ICT transition as predicted with the lower level of molecular orbital calculations.[14] On the other hand, the molecular orbitals involved in the visible absorption of Ap^- (mainly, the 40th and 42nd orbitals for the excited states) are distributed equivalently to the phenyl ring as well as the carbonyl

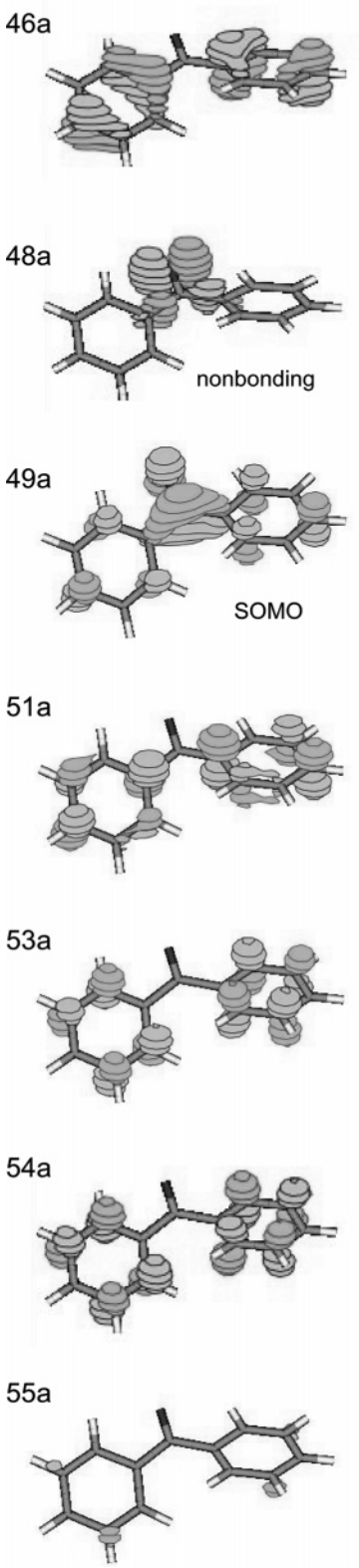

Figure 5. Outer valence molecular orbitals of the α spin space for the benzophenone radical anion.

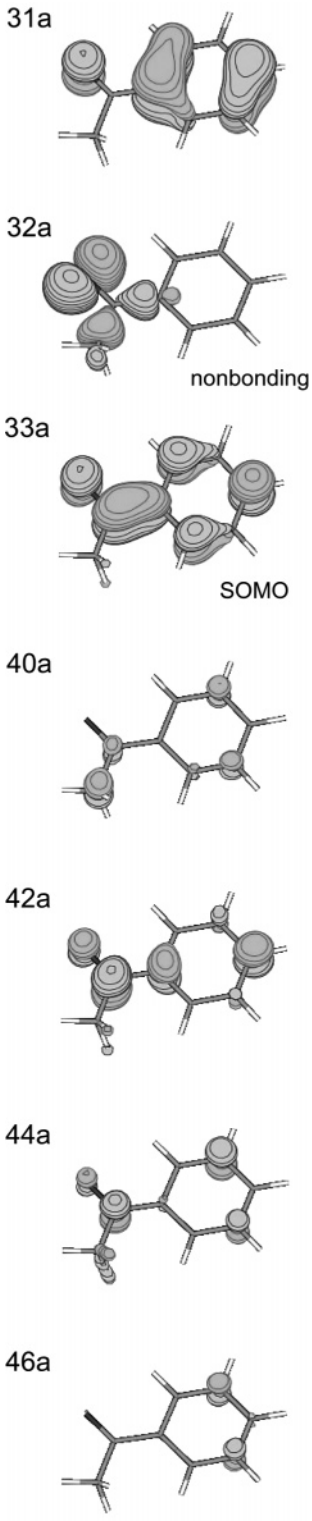

Figure 6. Outer valence molecular orbitals of the α spin space for the acetophenone radical anion.

group. Thus, the photoexcitation of Ap^- does not cause a significant change of the overall charge distribution.

Nature of the Methanol Coordination and the Spectral Shifts. Observed and calculated values of energetics for the present systems are summarized in Table 2. For Bp^- in the electronic ground state, the carbonyl group carries the largest negative charge, producing the significant stabilization by direct binding of solvent molecules. The binding energy between the carbonyl group and the solvents decreases in the excited state, where the excess electron delocalizes among the phenyl rings.

TABLE 1: Calculated Electronic Transitions to Bound Excited States for Bp^- and Ap^-

anion	transition energy (eV)	oscillator strength	excited state configuration[a]	coefficient
Bp^-	1.572	0.048	49α → 51α	−0.6498
			49α → 53α	0.7197
			49α → 55α	0.1732
	1.772	0.177	49α → 51α	0.6556
			49α → 53α	0.6786
			46β → 49β	−0.1177
	2.083	0.017	49α → 53α	−0.1703
			49α → 55α	0.9803
Ap^-	2.641	0.035	33α → 40α	0.9782
			33α → 42α	0.2007
	2.772	0.081	33α → 40α	−0.1498
			33α → 42α	0.9258
			31β → 33β	0.3746
	3.174	0.028	33α → 42α	−0.1026
			33α → 44α	0.9818
			31β → 33β	0.1627
	3.637	0.024	33α → 46α	0.9890
			31β → 33β	−0.1309

[a] $X\sigma$ denotes the Xth orbital of the σ spin space.

TABLE 2: Experimental and Calculated Energetics of $Bp^-\cdot(MeOH)_n$ and $Ap^-\cdot(MeOH)_n$

species	E_{exp} (eV)[a]	E_{calc} (eV)[b]	VDE_{calc} (eV)[c]	ΔE_{HB} (eV)[d]
Bp^-	1.43 ± 0.04	1.772 [0.177]	0.91	
$Bp^-\cdot MeOH$	1.61 ± 0.03	1.919 [0.147]	1.29	0.57
$Bp^-\cdot(MeOH)_2$	1.79 ± 0.04	2.062 [0.110]	1.65	0.50
$Bp^-\cdot(MeOH)_3$	1.82 ± 0.06	2.029 [0.104]	1.74	0.45
$Bp^-\cdot(MeOH)_4$	1.86 ± 0.07			
$Bp^-\cdot(MeOH)_5$	1.95 ± 0.06			
Ap^-	2.55 ± 0.03	2.772 [0.081]	0.52	
$Ap^-\cdot MeOH$	2.64 ± 0.09	2.849 [0.097]	1.03	0.66
$Ap^-\cdot(MeOH)_2$	2.73 ± 0.06	2.9413 [0.103]	1.42	0.54
$Ap^-\cdot(MeOH)_3$	2.74 ± 0.07	3.017 [0.086]	1.77	0.42
$Ap^-\cdot(MeOH)_4$	2.76 ± 0.04			

[a] Experimentally determined absorption peak values. [b] Calculated transition energies associated with the maximum oscillator strengths in brackets. [c] Calculated vertical electron detachment energies. [d] Energy difference between the sizes of n and $(n-1)$ clusters with the basis set superposition error (BSSE) corrections but regardless of the zero-point energy differences.

Therefore, as far as the electronic interaction of hydrogen bonds is concerned, the "first solvation shell" is completed when two molecules fill the coordination space around the carbonyl group. Attaching a surplus methanol molecule to form a hydrogen-bonded chain causes a much smaller difference in solvation energies between the two electronic states.

The DFT calculations for $Bp^-\cdot(MeOH)_n$ exhibited the out-of-plane coordination of methanol molecules around the carbonyl group, as shown in Figure 2. It has been believed for a long time that such geometries result from a strong hydrogen-bonding interaction with the SOMO (π^* orbital) localized on the anionic carbonyl group,[15,29] while nonbonding electrons on the oxygen atom bind to protic solvents in the neutral state. Further analyses on the results of the DFT calculations, however, give rise to a doubt about such an interpretation. In the optimized geometries of the $Bp^-\cdot(MeOH)_1$ cluster anions, the methanol molecules are not located just above or beneath the carbonyl group, where the dihedral angle with respect to the hydrogen bond (including C−C═O···H bonds) is only 26.2°. It does not seem to be in a significant order of difference with the corresponding quantity for the neutral state (16.7°). The nonbonding orbital is more localized on the carbonyl group in

comparison with the SOMO spread by the π-conjugation. Therefore, hydrogen bonding in the anionic state still has a dominant character of the nonbonding orbitals, and there is another reason why the out-of-plane coordination takes place in the anionic state. Upon the electron attachment to the benzophenone molecule, the geometric structure becomes more planar and the bond angle between the carbonyl and the two phenyl groups increases from 120.4° to 122.7°. As a consequence, the distance between the oxygen atom of the carbonyl group and the nearest hydrogen atom of the phenyl ring is shortened from 2.55 to 2.41 Å. This must shrink the coordination space on the horizontal side of the carbonyl group, and the solvent molecules are kicked out of the plane.

The dihedral angle of the hydrogen bonds in the optimized geometry for $Bp^-\cdot(MeOH)_2$ becomes close to vertical (68.8°), seeming that the bonding interaction with the SOMO enhances as the size increases. Nevertheless, the stepwise solvation energy (ΔE_{HB}) is calculated to slightly decrease when the second methanol molecule is attached. Thus, it can be concluded that the methanol coordination angle does not result from the specific interaction with the SOMO but from repulsive forces between the solvent molecules due to the congestion around the carbonyl group having a small coordination space. It is also concluded that the angle itself induces no significant change of the hydrogen bond strength leading to the spectral shifts. These conclusions bring a serious inconsistency with the previous interpretation on the temporal evolution of blue-shifts of transient absorption following pulse radiolysis,[9−12] which were attributed to the solvent reorientation from the in-plane to the out-of-plane geometries.[15,29]

It has been considered that the anions in the nascent state after pulse radiolysis already form hydrogen bonds with solvents keeping the stable orientation in the neutral state because it was assumed that the pulse radiolysis induces vertical electron attachment. The hypothesis of solvent reorientation has been grounded on experimental evidence that no spectral shift occurs in an alcoholic matrix at 4 K,[15] where the solvent motion was frozen. Perhaps the spectral shifts in the condensed phase should be analyzed from the aspect of deformation involving the *intramolecular* structure of the anion as well as the solvent reorientation because torsional motion of the phenyl rings might be considerably hindered at a very low temperature. As a further confirmation, Figure 7 shows simulated electronic spectra for $Bp^-\cdot(MeOH)_n$, $n = 0-3$, at the neutral and anionic optimized geometries. The torsional angle of the phenyl rings is found to keep within a deviation of 3° under the cluster formation in both the neutral and anionic geometries. Although the chain-forming geometry was calculated to be slightly more stable for $n = 2$ in the neutral state, we adopted the geometry of double coordination to maintain the coordination number through the deformation. The energy shifts between the main peaks for the two geometries of the bare and solvated anions are in the range of 0.34−0.43 eV, which makes a permissible agreement with the observed shifts in the transient absorption spectra. Because the clusters exhibit similar shifts to that of the bare anion, deformation of the intramolecular coordinates rather than the solvent orientations are responsible for the spectral shifts, assuming that the coordination number is unchanged throughout the dynamical process after pulse radiolysis. Otherwise, the transient spectral shifts can be recognized to originate from formation of additional hydrogen bonds if the inherent coordination number is less than two in the neutral solution phase, or if pulse radiolysis induces breakage of hydrogen bonds in a very short time scale.

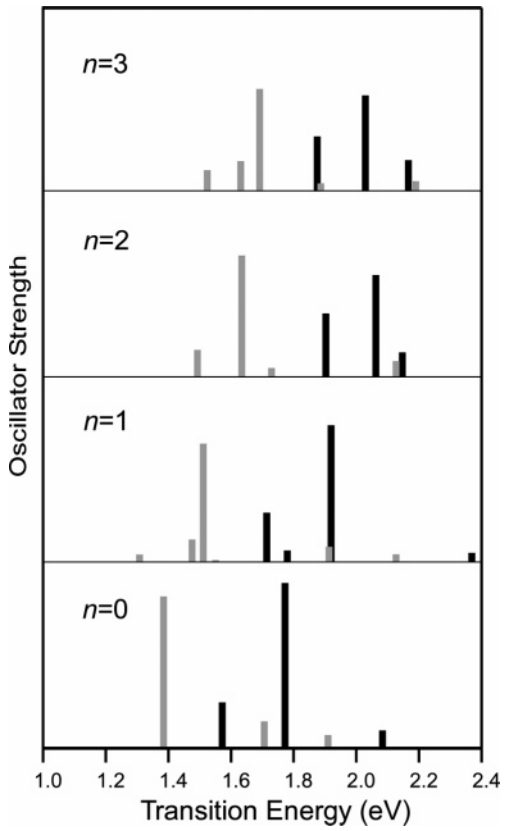

Figure 7. Simulated electronic spectra of $Bp^-\cdot(MeOH)_n$, $n = 0-3$ in the neutral (gray sticks) and anionic (black sticks) optimized geometries.

For the solvated Ap^- case, up to 3 of the coordination number around the carbonyl group were found in the calculation. The in-plane binding form is the most stable for $Ap^-\cdot(MeOH)_1$ in spite of negative charge density on the carbonyl group comparable with Bp^-. These differences should be caused by a less steric hindrance due to the methyl group instead of the phenyl group for the Bp^- case. However, a similar situation for interpretation of the observed spectra holds except for the small spectral shifts. It is easy to give a qualitative explanation for the small shifts by inspecting molecular orbitals shown in Figure 6. As mentioned above, the SOMO and the excited orbitals relevant to the visible absorption have comparable amplitudes both in the carbonyl and phenyl groups because of the effective π conjugation. Therefore, the small change of charge distribution does not significantly affect the solvation energy in the excited state, leading to the small spectral shift. This trend coincides with general formulations[30] given for the solvatochromic shifts of dipole transition of neutral molecules.

4. Conclusions

In this paper, we reported the PDE spectra of the bare and methanol-solvated radical anions of benzophenone and acetophenone. The B3LYP/6-31+G(d,p) level of calculations were performed to analyze the characteristic spectral shifts. A large solvatochromic shift for Bp^- is induced by a drastic change of electron distribution upon the electronic transition of the ICT character, while there is a small overall change for Ap^-. For both the ketyl anions, the shifts with two or three methanol molecules exhibit a near convergence on the bulk limit, which can be recognized as formation of the "first solvation shell" corresponding to the full coordination of solvents around the carbonyl group. The maximum coordination number is determined by the congestion around the carbonyl group. It is

responsible for the coordination angle of the solvents, which does not significantly affect binding energy as well as the spectral shifts. We proposed an alternative interpretation for the transient absorption spectra in the condensed phase that the relaxation of the intramolecular structure involving the phenyl torsion is more important to produce the spectral shifts than the solvent reorientation.

Combination of photoelectron spectroscopy with the present study will concrete the solvation energetics of the ketyl anions more apparently. Moreover, geometrical difference between the neutral and anionic states will be elucidated on the basis of the experimental evidence. However, we should note that vibrational analysis of the photoelectron spectrum must need a careful treatment with respect to the photon energy because there will be a strong resonance effect[31,32] from the excited states having a much larger transition cross-section than that for the direct electron detachment.

Acknowledgment. This work is partially supported by the Grant-in-Aid for Specifically Promoted Research (no. 16002006) from the Ministry of Education, Culture, Sports, Science, and Technology (MEXT) of Japan. T.M. thanks financial support by the Grant-in-Aid for Scientific Research (no. 17550006) from the Japan Society of the promotion of Science.

Supporting Information Available: Natural populations for benzophenone and acetophenone in the neutral and anionic states were calculated at the B3LYP/6-31+G(d,p) level. This material is available free of charge via the Internet at http://pubs.acs.org.

References and Notes

(1) Bachmann, W. E. *J. Am. Chem. Soc.* **1933**, *55*, 1179.
(2) Bachmann, W. E. *J. Am. Chem. Soc.* **1933**, *55*, 770.
(3) Pedersen, S. U.; Christensen, T. B.; Thomasen, T.; Daasbjerg, K. *J. Electroanal. Chem.* **1998**, *454*, 123.
(4) Elving, P. J.; Leone, J. T. *J. Am. Chem. Soc.* **1958**, *80*, 1021.
(5) Vauthey, E.; Pilloud, D.; Haselbach, E.; Suppan, P.; Jacques, P. *Chem. Phys. Lett.* **1993**, *215*, 265.
(6) Schaefer, C. G.; Peters, K. S. *J. Am. Chem. Soc.* **1980**, *102*, 7566.
(7) Hayon, E.; Ibata, T.; Lichtin, N. N.; Simic, M. *J. Phys. Chem.* **1972**, *76*, 2072.
(8) Hoshino, M.; Arai, S.; Imamura, M. *J. Phys. Chem.* **1974**, *78*, 1473.
(9) Marignier, J. L.; Hickel, B. *Chem. Phys. Lett.* **1982**, *86*, 95.
(10) Marignier, J. L.; Hickel, B. *J. Phys. Chem.* **1984**, *88*, 5375.
(11) Lin, Y.; Jonah, C. D. *J. Phys. Chem.* **1992**, *96*, 10119.
(12) Xujia, Z.; Lin, Y.; Jonah, C. D. *Radiat. Phys. Chem.* **1999**, *54*, 433.
(13) Shida, T.; Hamill, W. H. *J. Am. Chem. Soc.* **1966**, *88*, 1683.
(14) Shida, T.; Iwata, S.; Imamura, M. *J. Phys. Chem.* **1974**, *78*, 741.
(15) Ichikawa, T.; Ishikawa, Y.; Yoshida, H. *J. Phys. Chem.* **1988**, *92*, 508.
(16) Shida, T. *Electronic Absorption Spectra of Radical Ions*; Elsevier: Amsterdam, 1988.
(17) Maeyama, T.; Yagi, I.; Murota, Y.; Fujii, A.; Mikami, N. *J. Phys. Chem. A* **2006**, *110*, 13712.
(18) Maeyama, T.; Negishi, Y.; Tsukuda, T.; Yagi, I.; Mikami, N. *Phys. Chem. Chem. Phys.* **2006**, *8*, 827.
(19) Frisch, M. J.; Trucks, G. W.; Schlegel, H. B.; Scuseria, G. E.; Robb, M. A.; Cheeseman, J. R.; Montgomery, J. A., Jr.; Vreven, T.; Kudin, K. N.; Burant, J. C.; Millam, J. M.; Iyengar, S. S.; Tomasi, J.; Barone, V.; Mennucci, B.; Cossi, M.; Scalmani, G.; Rega, N.; Petersson, G. A.; Nakatsuji, H.; Hada, M.; Ehara, M.; Toyota, K.; Fukuda, R.; Hasegawa, J.; Ishida, M.; Nakajima, T.; Honda, Y.; Kitao, O.; Nakai, H.; Klene, M.; Li, X.; Knox, J. E.; Hratchian, H. P.; Cross, J. B.; Bakken, V.; Adamo, C.; Jaramillo, J.; Gomperts, R.; Stratmann, R. E.; Yazyev, O.; Austin, A. J.; Cammi, R.; Pomelli, C.; Ochterski, J. W.; Ayala, P. Y.; Morokuma, K.; Voth, G. A.; Salvador, P.; Dannenberg, J. J.; Zakrzewski, V. G.; Dapprich, S.; Daniels, A. D.; Strain, M. C.; Farkas, O.; Malick, D. K.; Rabuck, A. D.; Raghavachari, K.; Foresman, J. B.; Ortiz, J. V.; Cui, Q.; Baboul, A. G.; Clifford, S.; Cioslowski, J.; Stefanov, B. B.; Liu, G.; Liashenko, A.; Piskorz, P.; Komaromi, I.; Martin, R. L.; Fox, D. J.; Keith, T.; Al-Laham, M. A.; Peng, C. Y.; Nanayakkara, A.; Challacombe, M.; Gill, P. M. W.; Johnson, B.; Chen, W.; Wong, M. W.; Gonzalez, C.; Pople, J. A. *Gaussian 03*; Gaussian, Inc.: Wallingford, CT, 2004.
(20) Schaftenaar, G. *Molden 3.4*; CAOS/CAMM Center: Nijmegen, The Netherlands, 1998.
(21) Flükiger, P.; Lüthi, H. L.; Portmann, S.; Weber, J. *Molekel 4.3*, Swiss Center for Scientific Computing, Manno, Switzerland, 2002; http://www.cscs.ch/molekel/.
(22) Salyards, M. J.; Knight, W. B.; Grimsrud, E. P. *Int. J. Mass Spectrom.* **2003**, *222*, 201.
(23) Grimsrud, E. P.; Caldwell, G.; Chowdhury, S.; Kebarle, P. *J. Am. Chem. Soc.* **1985**, *107*, 4627.
(24) Chen, E. C. M.; Wentworth, W. E. *J. Phys. Chem.* **1983**, *87*, 45.
(25) Wentworth, W. E.; Kao, L. W.; Becker, R. S. *J. Phys. Chem.* **1975**, *79*, 1161.
(26) Schiedt, J;, Knott, W. J.; Le Barbu, K.; Schlag, E. W.; Weinkauf, R. *J. Chem. Phys.* **2000**, *113*, 9470.
(27) Born, M. *Z. Phys.* **1920**, *1*, 45.
(28) Rashin, A. A.; Honig, B. *J. Phys. Chem.* **1985**, *89*, 5588.
(29) Tachikawa, H. *J. Phys. Chem.* **1996**, *100*, 17090.
(30) McRae, E. G. *J. Phys. Chem.* **1957**, *61*, 562.
(31) Bailey, C. G.; Dessent, C. E. H.; Johnson, M. A.; Bowen, K. H., Jr. *J. Chem. Phys.* **1996**, *104*, 6979.
(32) Poliakoff, E. D.; Lucchese, R. R. *Phys. Scr.* **2006**, *74*, C71.